ELSEVIER

Chemical Engineering Journal 90 (2002) 139–147

Chemical Engineering Journal

www.elsevier.com/locate/cej

Study of the cracking reaction of linear and branched hexanes under protolytic conditions by non-stationary kinetics

V. Fierro [a], Y. Schuurman [b], C. Mirodatos [b,*], J.L. Duplan [a], J. Verstraete [a]

[a] *Institut Français du Pétrole, Centre d'Études et Développement Industriels (CEDI) 'René Navarre', F-69626 Villeurbanne Cédex, France*
[b] *Institut de Recherches sur la Catalyse, CNRS, 2 Avenue Albert Einstein, F-69626 Villeurbanne Cédex, France*

Abstract

The cracking reactions of C6 paraffins (*n*-hexane, 2-methylpentane, 3-methylpentane, 2,2-dimethylbutane and 2,3-dimethylbutane) over a fluidized catalytic cracking (FCC) catalyst at temperatures between 573 and 923 K have been studied in a temporal analysis of products (TAP) reactor. A mathematical model taking into account the extra- and intra-crystalline transport phenomena was used to describe the experimental data and allowed to determine the diffusion, sorption and intrinsic kinetic parameters for the hydrocarbons studied. These parameters are compared with published values obtained by independent methods. The sorption parameters increase with increasing branching in agreement with literature data while no variation of the diffusivity was observed. The activation energies for the overall disappearance of the C6 paraffins, containing contributions of dehydrogenation and C–C bond cleavage, vary only slightly with the degree of branching. The product distribution, however, varies greatly with the various isomers.

Keywords: Protolytic cracking; Temporal analysis of products; FCC catalysts; Kinetic modeling; Diffusion

1. Introduction

In a fluidized catalytic cracking (FCC) unit, heavy petroleum fractions are cracked to lower molecular weight products in the presence of an acid catalyst. The unit consists of two vessels: the riser-reactor, where almost all the endothermic reactions and coke deposition on the catalyst occur, and the regenerator, where air is used to burn coke. The regeneration process provides, in addition to reactivating the catalyst, the heat required to vaporize the liquid petroleum fraction entering the system and the enthalpy necessary to allow the endothermic cracking reactions.

Both thermal and catalytic cracking reactions take place in the riser and the reactor vessel. Thermal cracking reactions proceed via a radical chain of moderate length to produce, after a succession of cracking/recracking events, a product rich in C1 and C2 hydrocarbons and α-olefins [1]. The production of light gas is not commercially interesting, however. On the contrary, the main objective of FCC units is the production of hydrocarbons in the gasoline region (C5–12, 20–221 °C boiling range), while other commercially important products are LPG (a blend of C3 and C4 hydrocarbons) and light cycle oil (C13–20).

It has been established that the catalytic cracking of a paraffin proceeds via two mechanisms occurring in a concerted manner [2–8]. It is believed that the initiation step in the cracking of paraffins on solid acids is a monomolecular step that involves the attack of a proton from a strong Brönsted acid site on either a C–C or a C–H bond. This yields a pentacoordinated carbonium ion that evolves by protolysis leading to either a shorter paraffin and the complementary adsorbed carbenium ion, or to H_2 while leaving behind a carbenium ion of the original reactant. The resulting carbenium ion adsorbed on the surface can either desorb as an olefin, undergo rearrangements into isomers, crack through β-scission (a second cracking mechanism), or be saturated through a hydride transfer step from a reactant molecule.

In the case of isobutane, the difference between the initiation and propagation were unambiguously established by Corma et al. [9] and a reaction scheme for the cracking of this molecule was reported. It was shown that H_2 and CH_4 could only be produced by the initiation steps and that all the paraffins were only produced by propagation reactions. Working at temperatures between 673 and 773 K, they determined that at lower cracking temperatures, 673–723 K, the controlling step is the bimolecular chain hydride transfer. However, at higher temperatures, 723–773 K the controlling step is the protolytic cracking. In FCC units, the temperature is between 773 and 823 K and protolytic cracking reactions would, therefore, be dominant. Similar results were found

* Corresponding author. Tel.: +33-472-44-5366; fax: +33-472-44-5399.
E-mail address: mirodato@catalyse.univ-lyon1.fr (C. Mirodatos).

1385-8947/02/$ – see front matter
PII: S1385-8947(02)00075-X

for hexane molecules by Bassir and Wojciechowsky [10] and for methylhexane by Bamwenda et al. [11].

In FCC operations, light gases have usually been supposed to result from thermal cracking. Most studies in literature do not take into account thermal cracking when determining the cracking kinetics in micro activity test (MAT) reactors because the reaction temperature is not supposed to allow these reactions in a meaningful extent. Temporal analysis of products (TAP) experiments offer several advantages to the study of catalytic cracking over zeolites or FCC catalysts. They allow the determination of catalytic cracking kinetics free from thermal cracking due to the low pressures applied. The amount of product pulsed is small compared to the amount of catalyst and, therefore, the coking of the catalyst remains negligible during the experiments. At low pressures, bimolecular reactions are suppressed and, thus, the monomolecular protolytic cracking route can more easily be investigated, even at high conversions, as was demonstrated for the cracking of methylcyclohexane [12]. Moreover, TAP experiments give access to the diffusion inside the micropores, sorption and intrinsic kinetic parameters [13–15].

In this work, the cracking of C6 paraffins over industrial FCC catalysts has been studied in a TAP reactor to investigate the effect of branching on the sorption, diffusion and reaction.

2. Experimental

2.1. Catalyst

In this study, an industrial FCC catalyst was used. Its main characteristics are presented in Table 1. It consists of Y-zeolite, a silica–alumina matrix and a binder. It was pretreated prior to evaluation by an ex situ hydrothermal treatment at 1043 K for 15 h using 100% steam. For the physicochemical characterization, XRD (unit-cell size, relative cristallinity), XRF (aluminum, silicon and rare earth and metal content), N_2 ad/desorption and Hg intrusion (S_{BET} and pore volume) measurements were done.

Table 1
Characterization of the FCC catalyst used

XRF	Overall Si/Al (wt/wt)	1.51
	Rare earth (wt.%)	1.153
	K (wt.%)	0.058
	Fe (wt.%)	0.366
	Ti (wt.%)	0.859
	P (wt.%)	0.047
	Ni (wt.%)	0.0
	V (wt.%)	0.0
XRD	Unit cell size (Å)	24.31
Physical analysis	S_{BET} ($m^2\,g^{-1}$)	138
	Skeletal density ($g\,cm^{-3}$)	2.63
	Volume Hg ($cm^3\,g^{-1}$)	0.75
	Particle density ($g\,cm^{-3}$)	0.86
	Pore volume ($cm^3\,g^{-1}$)	0.78

The X-ray diffractograms were measured with a step scan of $0.25^\circ\,min^{-1}$ using Cu Kα-radiation (0.15418 nm) at 40 kV/30 mA. Silicon powder was added as an internal standard (0.05 g for 1.5 g of catalyst) and the samples were prepared as self-supporting wafers. The catalyst has an unit cell size of 24.31 Å calculated according to the ASTM-method D3942-41 and was constituted in an important fraction of amorphous material, indicating a partial destruction of the zeolite.

The XRF measurements were carried out using a Philips PW 1480 spectrometer with Cr Kα-radiation and 50 mV/50 mA. The measured lines were Al Kα, Si Kα, Ti Kα, Fe Kα, Ni Kα, V Kα, P Kα, La Kα, Ce Kα, Pr Lβ and Nd Lβ. For the measurements, the samples were prepared by melting the catalyst sample with tetraboric acid into a pearl. A Si/Al weight ratio of 1.51 was determined.

The BET surface area was measured with a Micromeritics ASAP 2400 by ad/desorption of N_2 at the liquid nitrogen boiling temperature. The pore volume was determined by mercury porosimetry with a Micromeritics AutoPore 9420. Prior to the measurements the samples were degassed at 573 K for 12 h.

2.2. TAP experiments

The TAP-2 reactor system was used to perform transient response experiments under vacuum and at temperatures ranging from 573 to 923 K. *n*-Hexane, 2-methylpentane, 3-methylpentane, 2,2-dimethylbutane and 2,3-dimethylbutane were obtained from Aldrich (99.9% purity) and used without further purification. Neon was used as an internal standard for calibration and as a reference for diffusion. The reactant hydrocarbons together with neon were introduced in the microreactor (25.4 mm in length and 4 mm in diameter) in a volume ratio of 1:1. The reactor is evacuated continuously and the response of these pulses as a function of time was recorded by a quadrupole mass spectrometer located directly underneath the reactor exit. For details of this technique, the reader is referred to Gleaves et al. [16].

A catalyst loading of 100 mg with a particle size of approximately 0.1 mm was placed in the center of two layers of 0.2–0.3 mm size quartz particles. A microreactor filled with quartz only was employed to determine the Knudsen diffusion coefficients. The transient responses of the C6 isomers were monitored by a quadrupole mass spectrometer following the signal of a single atomic mass unit (amu) per pulse as a function of time. The C6 isomers were monitored on the amu 86, 71 and 57. The amu's of 58, 44, 30, 16 and 2 were also monitored as they correspond to the possible main products of the monomolecular cracking (butane, propane, ethane, methane and hydrogen) and the C6 isomers give negligible contributions to these fragments (<5%). During the experiments, the pulses were repeated several times and the absence of deactivation could, therefore, be verified.

2.3. Modeling

The zeolite particles are modeled as squared slabs with a characteristic length L_z located in the macropores of the silica–alumina matrix. These particles are considered to be symmetrical. Reversible sorption takes place at the exterior of zeolite particles and is described by an equation analogous to Henry's law:

$$C_{A,z}|_{z=l/2} = H' C_A \quad (1)$$

where H' is the analogous Henry coefficient ($m_g^3\, m_s^{-3}$), C_A the reactant concentration ($mol\, m^{-3}$) and z the zeolite coordinate (m). Only the adsorbed molecules diffuse into the micropores. During TAP experiments, the concentration in the reactor remains very low and, therefore, the diffusion in the zeolite pores is assumed to be independent of the concentration and is, therefore, described by Fick's law. Inside the pores, first-order irreversible reaction takes place on the acid sites.

The reactor is divided into three zones: two inert zones of quartz beads between which the catalyst is placed. The diffusion in all three zones is described by Knudsen diffusion. In the catalyst zone, the flux into the catalyst particles is included in the model. Actually, the zeolite particles are located within a macroporous matrix. However, the diffusion into the macropores is relatively fast and can, therefore, be lumped into the Knudsen diffusion coefficient according to the following equation [17]:

$$D_{K,p} = \frac{D_K}{1 + (\varepsilon_p(1-\varepsilon_b))/\varepsilon_b} \quad (2)$$

where D_K is the Knudsen diffusivity in the bed ($m^2\, s^{-1}$), $D_{K,p}$ the Knudsen diffusivity in the pores of the particle ($m^2\, s^{-1}$), ε_p the particle porosity ($m_g^3\, m_s^{-3}$) and ε_b the bed porosity ($m_g^3\, m_r^{-3}$). This leads to the following continuity equation for the catalyst zone:

$$\varepsilon_b \frac{\partial C_A}{\partial t} = D_{K,p} \frac{\partial^2 C_A}{\delta x^2} - (1-\varepsilon_b) a_z J_{A,z} \quad (3)$$

where t is the time (s), x the reactor coordinate (m), a_z the zeolite surface area per volume ($m^2\, m^{-3}$) and $J_{A,z}$ ($mol\, m^{-2}\, s^{-1}$) is the molar flux into the zeolite as given by Eq. (3):

$$J_{A,z} = D_{z,eff} \frac{\partial^2 C_{A,z}}{\partial z^2} \quad (4)$$

where $D_{z,eff}$ is the effective Knudsen diffusivity ($m^2\, s^{-1}$) in the zeolite. The continuity equation for the diffusion inside the micropores is analogous to Eq. (3) with an effective diffusion coefficient and it contains a term accounting for irreversible cracking.

$$\varepsilon_z \frac{\partial C_{A,z}}{\partial t} = D_{z,eff} \frac{\partial^2 C_{A,z}}{\delta z^2} - (1-\varepsilon_z) N_z k_r C_{A,z} \quad (5)$$

where $N_{z,eff}$ is the number of acid sites ($mol\, m^{-3}$) and k_r the rate coefficient for the irreversible cracking reaction ($m^3\, mol^{-1}\, s^{-1}$).

The initial and boundary conditions for TAP experiments are reported in [16]. The additional boundary conditions for this model is Eq. (1). The model has already been described in reference [15] and similar models to describe diffusion in microporous materials have been employed by Keipert and Bearns [13] and Nijhuis et al. [14].

Parameter estimation was performed by fitting the entire simulated response curve to the experimental one in the time domain. For each curve, the sum of the squared deviations over 400 data points was used as the objective function which was minimized using an algorithm based on Marquardt's method [18]. Diffusion and sorption parameters were determined simultaneously by matching the simulated response curves of the hydrocarbons to the experimentally obtained ones at low temperatures between 523 and 673 K where no reaction takes place. The kinetic parameters were estimated from the response curves at temperatures from 773 to 923 K, fixing the diffusion and sorption parameters at the values determined at low temperatures.

For the regression analysis, a reparameterized form of the Arrhenius and Van't Hoff equations was used. A full statistical analysis, which included the calculation of the 95% confidence intervals on the estimated parameters, was performed after regression.

3. Results and discussion

Preliminary experiments were carried out by pulsing the hexane isomers over quartz at temperatures up to 1098 K. These experiments showed no conversion of any of the reactants indicating that thermal cracking reactions can be excluded under TAP conditions.

Fig. 1 shows the experimental response curves when pulsing 2,2-dimethylbutane at temperatures between 573 and 923 K over the industrial FCC catalyst. Up to 723 K, no reaction was observed and the change in pulse shape with increasing temperature is due to the change in diffusion and sorption parameters (Fig. 1a). At higher temperatures (Fig. 1b), part of the 2,2-dimethylbutane cracks irreversibly, leading to more narrow pulse responses. Similar transient responses as a function of temperature were observed for all hexane isomers.

The mass spectrometry analysis only allows a rather crude quantification of butane, propane, ethane, methane and hydrogen during these experiments. No significant amounts of ethane and butane were observed. Product yields were calculated as the ratio between the amount of the product formed and the amount of C6 isomer pulsed. Fig. 2a–c show the yield of propane, methane and hydrogen for all the hexane isomers at temperatures between 773 and 923 K. No analysis was made of the olefin production or the formation of heavier fractions. From the data presented in Fig. 2, a

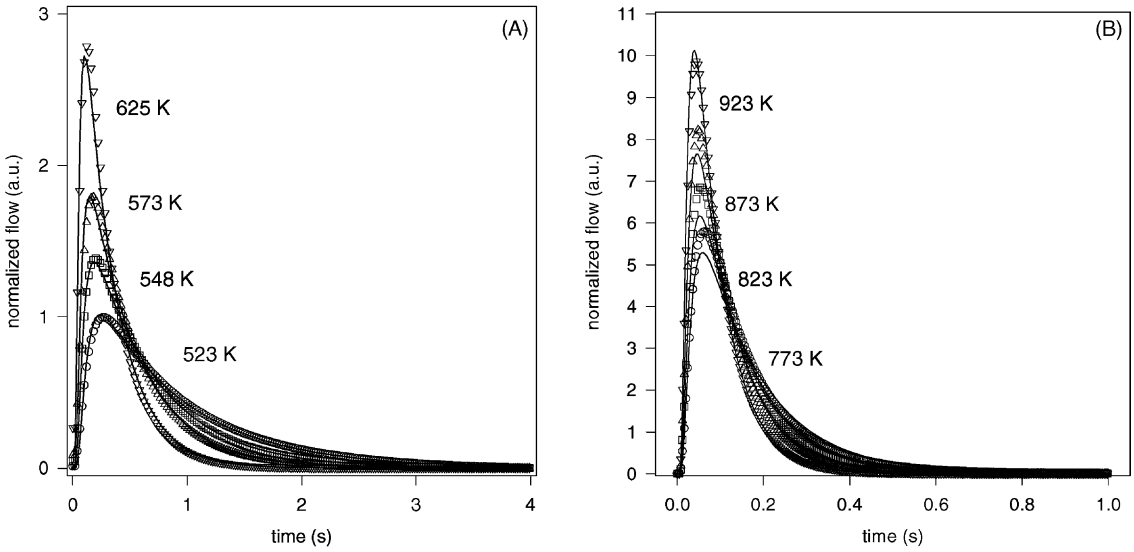

Fig. 1. Experimental and model response curves for 2,2-methylbutane pulses at temperatures (a) from 573 to 723 K and (b) from 773 to 923 K.

carbon mass balance was calculated, assuming that all light hydrocarbons and hydrogen originated from protolytic cracking of the hexane isomer and that no consecutive reactions took place. At 923 K, this resulted in a 10% excess carbon balance for 2,2-dimethylbutane and 2,3-dimethylbutane, a closed carbon balance for 2-methylpentane, and a 10–15% carbon deficit in the case of 3-methylpentane and *n*-hexane (the latter being calculated at 873 K).

The considerable formation of light hydrocarbons and hydrogen results from the protolytic cracking of the hexane isomers, as no thermal cracking was observed during the preliminary experiments. The reaction conditions of the TAP reactor, i.e. low pressures and a high catalyst to reactant ratio, favor the protolytic cracking route, as was demonstrated for the cracking of methylcyclohexane [12].

From Fig. 2, it is clear that the product distribution strongly depends on the hexane isomer. 2,3-Dimethylbutane is the most reactive isomer yielding mainly propane and hydrogen. This can be explained by considering the formation of the carbonium ions. Protonating the central C–C bond of 2,3-dimethylbutane results in a carbonium ion that easily forms propane. Alternatively, a protonation on the second or third carbon atom of 2,3-dimethylbutane also leads to a stable carbonium ion. Splitting off hydrogen results in the formation of a tertiary carbenium ion, while splitting of a methane molecule yields a secondary carbenium ion. As tertiary carbenium ions are more stable than secondary ions, the production of hydrogen from 2,3-dimethylbutane is more important.

2,2-Dimethylbutane mainly yields methane and to a lesser extent propane, but no hydrogen. The formation of a carbonium ion on the second carbon atom will lead to a tertiary carbenium ion and methane or ethane, but can not result in the formation of hydrogen. Only traces of ethane were observed for 2,2-dimethylbutane. Propane, however, can not be explained by a direct protolytic cracking of 2,2-dimethylbutane. The transient responses showed the formation of propane after the appearance of methane and can, thus, be the result of secondary reactions. This also explains the excess in the carbon balance for 2,2-dimethylbutane as secondary reaction products should not be included in this balance.

3-Methylpentane and 2-methylpentane can form tertiary carbenium ions by splitting off hydrogen from the carbonium ion or form a secondary carbenium ion by cleavage of the C–C bond to give methane, ethane or propane. Again, the formation of the tertiary carbenium ion is preferred, as shown by the preponderant hydrogen production.

For *n*-hexane, there is no preferential formation of a specific carbonium ion and, hence, no particular product formation is favored. The deficit in the carbon balance also indicates that secondary reactions occur, for example the production of olefins that are not included in our analysis.

Bassir and Wojciechowski [10] found that the rupture of the propyl group was the most important protolytic reaction followed by the butyl group for all the C6 molecules except for 2,2-dimethylbutane. They also found that *n*-hexane showed the greatest tendency to protolysis whereas 2,3-dimethylbutane was resistant to all forms of protolysis, as compared to conversion by chain processes. From our results under TAP reaction conditions, it has been clearly established that hydrogen and methane are the main products (except for *n*-C6 where the production of hydrogen, methane and propane are comparable) and that the hydrocarbons crack more easily with increasing degree of branching. A direct comparison of the results obtained in both works is difficult due to the very different operating conditions. As Bassir and Wojciechowski worked at temperatures <773 K, it is possible that their results were influenced by the presence of mechanisms other than simple

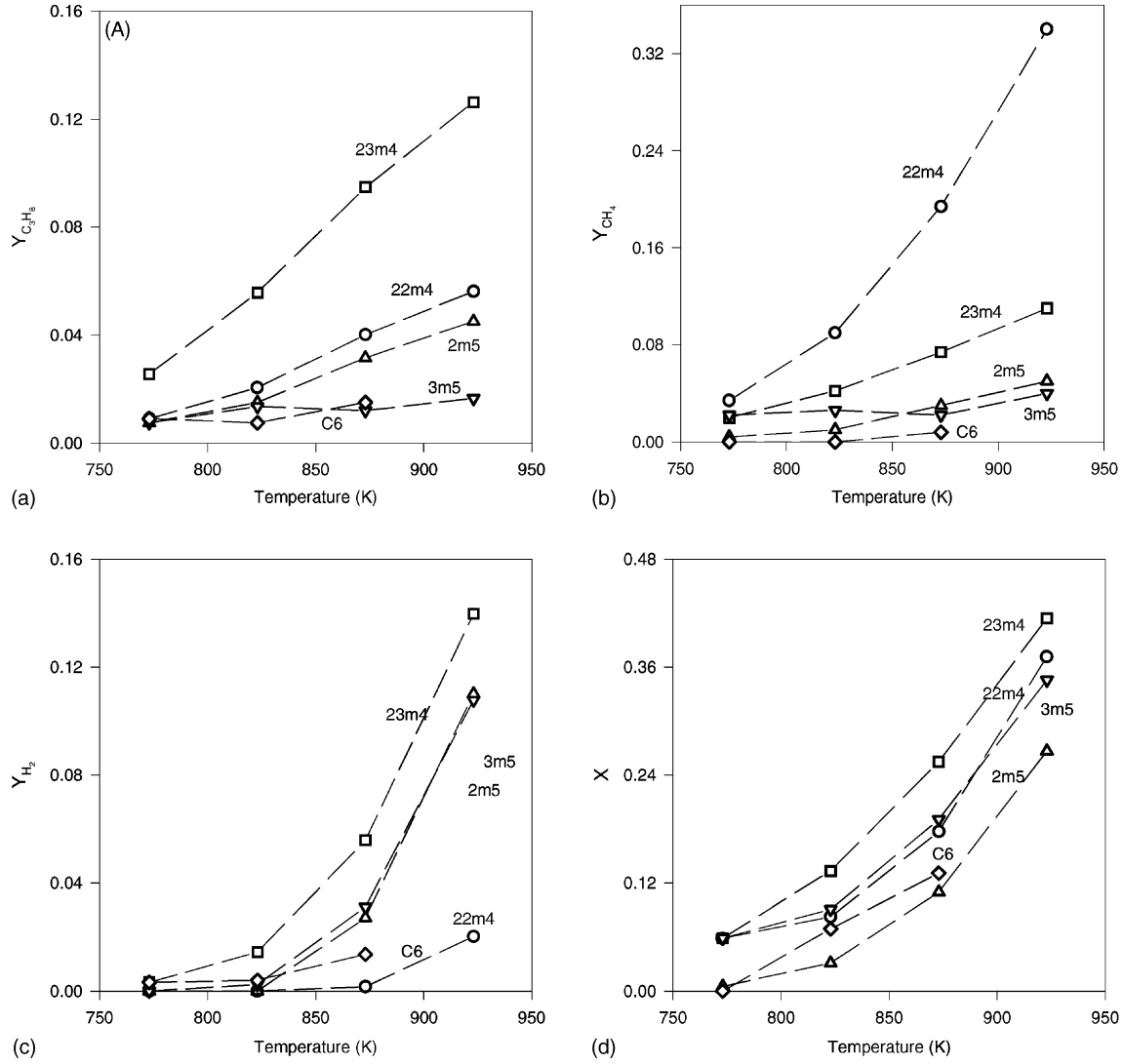

Fig. 2. Evolution with the temperature of the yield to (a) propane, (b) methane, (c) hydrogen and (d) the feed conversion reached. (*n*-Hexane: C6, 2-methylpentane: 2m5, 3-methylpentane: 3m5, 2,2-methylbutane: 22m4, 2,3-methylbutane: 23m4).

protolysis. On the other hand, their approach assumes initial selectivities, while our results were obtained at conversion levels up to 40% in the TAP reactor, as shown in Fig. 2d.

The diffusion, sorption and kinetic parameters of linear and branched C6 molecules were modeled from the transient responses of the hexane isomers. Fig. 1a shows the experimental and model responses for 2,2-dimethylbutane at temperatures between 573 and 723 K. The model describes the data adequately for all isomers. The Knudsen diffusivities for the extraparticle transport were determined from independent experiments. Hence, the model applied in this temperature range has only four adjustable parameters: the diffusivity in the micropores, the Henry coefficient for reversible sorption on the zeolite particles, the activation energy for the diffusivity and the adsorption enthalpy. The data did not permit an estimation of the activation energy for the micropore diffusion significantly different from zero. It was, therefore, fixed at a low value of 10 kJ mol^{-1} taken as an average of the smaller activation energy values (see Table 5). The other parameter estimates together with their 95% confidence interval are presented in Table 2. The adsorption entropy reported in Table 2 is calculated from the Langmuir adsorption equilibrium coefficient with 1 bar as reference. At low pressures, the following relation exists between the analogous Henry coefficient, H', and the Langmuir adsorption equilibrium coefficient, K (Pa^{-1}):

$$H' = RTKq_{sat} \quad (6)$$

where q_{sat} (mol m$_{cat}^{-3}$) is the hexane saturation adsorption concentration.

The kinetic parameters were obtained from the transient responses at temperatures between 773 and 923 K. In this case, all diffusion and sorption parameters were fixed at the values estimated from experiments at lower temperatures.

Table 2
Adsorption, diffusion and kinetic parameters for linear and branched C6 isomers

	ΔS[a] ($J\,mol^{-1}\,K^{-1}$)	ΔH_{ads} ($kJ\,mol^{-1}$)	K (823 K) (bar^{-1})	D° ($m^2\,s^{-1}$)	E_{diff}[b] ($kJ\,mol^{-1}$)	D (823 K) ($m^2\,s^{-1}$)	k°[b] (s^{-1})	E_{act} ($kJ\,mol^{-1}$)	k_r (823 K) (s^{-1})
n-Hexane	−78 ± 2	−42.6 ± 0.5	0.044	$1.6 \pm 0.5\ 10^{-10}$	10	3.7×10^{-11}	1×10^{7}	186.0 ± 1	1.6×10^{-5}
2-Methylpentane	−75 ± 2	−43.9 ± 0.5	0.074	$2.2 \pm 0.7\ 10^{-10}$	10	5.1×10^{-11}	1×10^{7}	188.9 ± 1	1.0×10^{-5}
3-Methylpentane	−75 ± 2	−44.2 ± 0.5	0.077	$2.4 \pm 0.8\ 10^{-10}$	10	5.6×10^{-11}	1×10^{7}	183.8 ± 1	2.2×10^{-5}
2,2-Dimethylbutane	−63 ± 2	−37.5 ± 0.5	0.123	$2.5 \pm 0.8\ 10^{-10}$	10	5.8×10^{-11}	1×10^{7}	180.0 ± 1	3.8×10^{-5}
2,3-Dimethylbutane	−65 ± 2	−40.2 ± 0.5	0.143	$6.1 \pm 0.7\ 10^{-11}$	10	1.4×10^{-11}	1×10^{7}	179.3 ± 1	4.2×10^{-5}

[a] Calculated assuming the C6 saturation concentration to be $200\,mol\,m^{-3}$.
[b] Fixed.

Only two adjustable parameters were taken into account: the pre-exponential factor lumped with the active site concentration and the activation energy for the first order irreversible cracking reaction. These two parameters appeared to be strongly correlated ($\rho = 0.995$) and, therefore, the pre-exponential factor was fixed at $10^7\ s^{-1}$ for all hexane isomers studied. This value corresponds to the pre-exponential factor calculated by Dumesic et al. [19] for the protolytic cracking of isobutane over Y-zeolites. The model was also run with values for the pre-exponential factor set at 10^6 and $10^8\ s^{-1}$ and adjusting the activation energy. This resulted in a less adequate fit. The activation energies, thus, estimated are reported in Table 2. A typical example of the model fit is given in Fig. 1b for 2,2-dimethylbutane.

3.1. Sorption parameters

Similar adsorption enthalpies were determined for *n*-hexane and the two methylpentanes. In contrast, significantly lower adsorption enthalpies were found for the two dimethylbutanes. The presence of two methyl groups reduces the interaction with the surface. A similar trend is observed for the condensation enthalpy of the hexane isomers as presented in Table 3. The enthalpy of condensation decreases with increasing branching of the hexane molecule. The absolute values of the adsorption enthalpies correspond very well with the values calculated according to an approach proposed by Sowerby et al. [20] and reported in Table 3. Table 4 lists the experimentally determined adsorption enthalpy of various C6 isomers over different zeolites reported by several authors. The absolute values found in this work are slightly lower than the range of values reported in Table 4.

Table 3
Variation of the entropy and enthalpy for condensation and adsorption of C6 isomers (ΔH_{theo}: adsorption enthalpies calculated by Sowerby et al. [20] approach, entropy and enthalpy of condensation [42])

	ΔS_{cond} ($J\,mol^{-1}\,K^{-1}$)	ΔH_{cond} ($kJ\,mol^{-1}$)	ΔH_{theo} ($kJ\,mol^{-1}$)
n-Hexane	−92	−31.6	−46.1
2-Methylpentane	–	−30.0	−44.9
3-Methylpentane	−90	−30.4	−44.5
2,2-Dimethylbutane	−86	−29.2	−42.3
2,3-Dimethylbutane	–	−27.8	−43.7

The variation of the adsorption entropy is more pronounced and similar to that of the adsorption enthalpy. The adsorption entropy decreases with increasing degree of branching of the isomer. Again an analogy can be found in the entropy of condensation, reported in Table 3. The more branched molecules retain more degrees of freedom upon adsorption (or condensation) compared to *n*-hexane. The absolute value of the adsorption entropies obtained from this study are lower than the values reported in the literature (between −80 and $-160\,J\,mol^{-1}\,K^{-1}$) for the adsorption of *n*-alkanes on MFI and FAU type zeolites [22]. This could be due to an underestimation of the hexane saturation concentration of $200\,mol\,m^{-3}$.

Overall, the adsorption coefficient, calculated from the adsorption enthalpy and the adsorption entropy, increases with increasing degree of branching, as shown in Table 2 for a temperature of 823 K. This illustrates that the variation of the adsorption entropy with the degree of branching determines the variation of the adsorption coefficient.

3.2. Diffusivity

The micropore diffusivity does not vary significantly with the degree of branching of the hexane molecule. A decrease of the diffusion coefficient with increasing degree of branching of C6 molecules has been reported by Cavalcante and Ruthven [23] and by Boulicaut et al. [24] in silicalite and by Schumacher et al. [25] for 2-methylpentane and *n*-hexane in MFI zeolites. The Y-zeolite is characterized by a more open structure than the MFI types giving fewer constraints to the diffusion of branched C6 molecules. The values determined in this work fall in the rather large range of those found by other authors as listed in Table 5.

3.3. Kinetic parameters

The activation energy reported in Table 2 corresponds to the disappearance of the C6 molecule and so it includes both protolytic dehydrogenation and C–C bond cleavage. The activation energy varies little for the different hexanes studied, although rather different product distributions have

Table 4
Comparison of experimental data for the adsorption of C6 isomers

	ΔH_{ads} (kJ mol^{-1})	Method	T	Sorbent	Reference
n-Hexane	−66	Gravimetry/calorimetry	363	ALPO-11/	[21]
	−65	Gravimetry/calorimetry	363	ZSM-5	[21]
	−53	Gravimetry/calorimetry	323	H-EMT	[22]
	−47	Gravimetry/calorimetry	323	FAU	[22]
	−43	TAP	573–773	USHY	This work
2-Methylpentane	−66	Gravimetry/calorimetry	363	ALPO-11	[21]
	−44	TAP	573–773	USHY	This work
3-Methylpentane	−57	Gravimetry/calorimetry	363	ALPO-11	[21]
	−62	Gravimetry/calorimetry	363	ZSM-5	[21]
	−44	TAP	573–773	USHY	This work
2,2-Methylbutane	−38	TAP	573–773	USHY	This work
2,3-Methylbutane	−40	TAP	573–773	USHY	This work

been observed depending on the hydrocarbon involved. In order to get more insight on the importance of the protolytic dehydrogenation and the C–C bond cleavage, the formation of the main products was modeled for the cracking of the two dimethylbutanes.

The transient responses for the production of methane from 2,2-dimethylbutane could be described adequately with the same pre-exponential factor and the same activation energy as for the disappearance reaction of 2,2-dimethylbutane. An adsorption enthalpy of 10 kJ mol^{-1} for the methane adsorption was assumed and the methane micropore diffusivity was found to have no influence on the overall fit. Fig. 3 shows the experimental and model response curves for the methane production from 2,2-dimethylbutane. Hence, the activation energy reported in Table 2 for 2,2-dimethylbutane corresponds to the breaking of the C–C bond in the carbonium ion transition state yielding methane and an adsorbed tertiary carbenium ion intermediate.

In the case of 2,3-dimethylbutane, both the hydrogen and the propane production have been modeled. The results are shown in Fig. 4a and b. Up to temperatures of 873 K, the hydrogen production can be described satisfactorily by the model. The effect of reaction temperature on the hydrogen production is slightly overestimated by the model, however. The activation energy for the formation of hydrogen amounted to 150 kJ mol^{-1}, a value significant lower than

Table 5
Comparison of experimental data for the diffusivity of C6 isomers

	D (T = 413 K) (cm^2 s^{-1})	E_{diff} (kJ mol^{-1})	Method	T (K)	Sorbent	Reference
n-Hexane	1–1.5 × 10^{-8}	17 ± 4	STFR	325–444	MFI	[26]
	4.0 × 10^{-8}	19	ZLC	334	MFI	[27]
	2.7 × 10^{-6}	8	PFG-NMR	298–473	MFI	[28]
	8.0 × 10^{-6}	5	QENS	373–453	MFI	[29]
	1.8–5 × 10^{-8}	7–16	Micro FTIR	398–473	MFI	[30]
	4.0 × 10^{-5}	22 ± 2.1	FR	273–473	MFI	[31]
	7.0 × 10^{-8}	19 ± 3	TEX-PEP	373–473	MFI	[25]
	1.9 × 10^{-8}	25	Gravimetry	363–433	Silicalite	[32]
	2.8 × 10^{-8}	36	Cromatography	363–433	Silicalite	[32]
	8.7 × 10^{-8}	10	TAP	573–773	HUSY	This work
2-Methylpentane	1.0 × 10^{-8}	29 ± 3	TEX-PEP	373–473	MFI	[25]
	5.0 × 10^{-9}	35	Gravimetry	297–338	MFI	[33]
	1.5 × 10^{-8}	46	Gravimetry	373–473	MFI	[23]
	1.2 × 10^{-8}	24	TAP	475–598	MFI	[13]
	1.7 × 10^{-8}	46	Gravimetry	363–433	Silicalite	[32]
	5.8 × 10^{-9}	27	Cromatography	363–433	Silicalite	[32]
	1.2 × 10^{-7}	10	TAP	573–773	HUSY	This work
3-Methylpentane	4.6 × 10^{-9}	46	Gravimetry	363–433	Silicalite	[32]
	2.2 × 10^{-9}	28	Cromatography	363–433	Silicalite	[32]
	1.3 × 10^{-7}	16	TAP	573–773	HUSY	This work
2,2-Methylbutane	1.4 × 10^{-7}	10	TAP	573–773	HUSY	This work
2,3-Methylbutane	3.3 × 10^{-8}	10	TAP	573–773	HUSY	This work

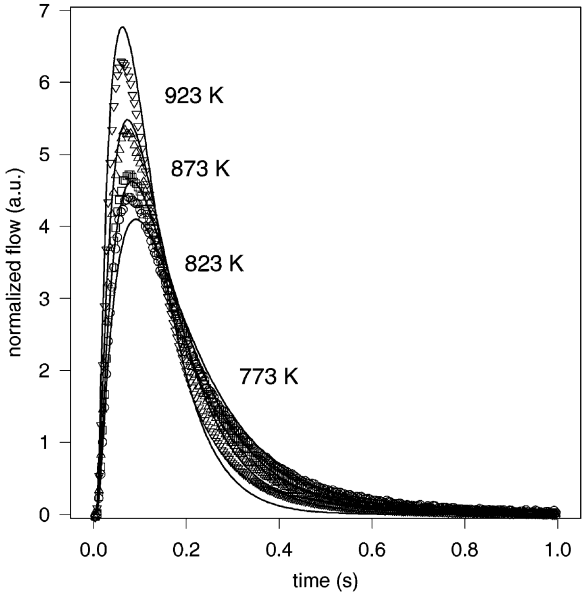

Fig. 3. Experimental and model response curves for methane produced during 2,2-methylbutane cracking from 773 to 923 K.

the activation energy of 180 kJ mol^{-1} for the disappearance reaction of 2,3-dimethylbutane. This fits in well with the work of Lercher et al. [34] who propose two different transition states for C–C bond breaking and dehydrogenation with experimentally observed activation energies of 200 and 160 kJ mol^{-1}, respectively, for the conversion of *n*-butane over HZSM5. At 923 K, the total amount of hydrogen is underestimated by the model and the tailing observed on the experimental curve is not accounted for by the model. This indicates that a part of the hydrogen produced at higher temperatures stems from secondary protolytic cracking reactions, which explains the excess in the carbon balance at high temperatures for 2,3-dimethylbutane. The model is not able to properly describe the propane production from 2,3-dimethylbutane at all temperatures applied. The transient response for propane seems to have two distinct time constants, an initial sharp peak followed by a long slow process (tailing). This response seems to indicate a slow desorption process of the propane as rate limiting step.

Table 6
Apparent activation energy of *n*-hexane and 2-methylpentane at protolytic cracking conditions

	E_{app} (kJ mol^{-1})	T (K)	Zeolite	Reference
n-Hexane	105		HZSM-5	[35]
	125		HZSM-5	[36]
	149	753–813	HZSM-5	[37]
	30–90		MFI with various Al contents	[38]
	142		USHY	[39]
	177	753–813	USHY	[37]
	141	773–873	USHY	[40]
	143	573–923		This work
2-Methylpentane	157	673–773	HY	[5]
	205	673–773	USHY	[10]
	151	673–773	USHY	[41]
	145	573–923	USHY	This work

The apparent activation energy usually reported, E_{app}, can be separated out into its constituent elements, namely, the intrinsic activation energy, E_{app}, and the adsorption enthalpy, ΔH_{ads}:

$$E_{act} = E_{app} - \Delta H_{ads} \quad (7)$$

Apparent activation energies determined in this study are in the range of 140–150 kJ mol^{-1}, well within the range of values given in literature and listed in Table 6.

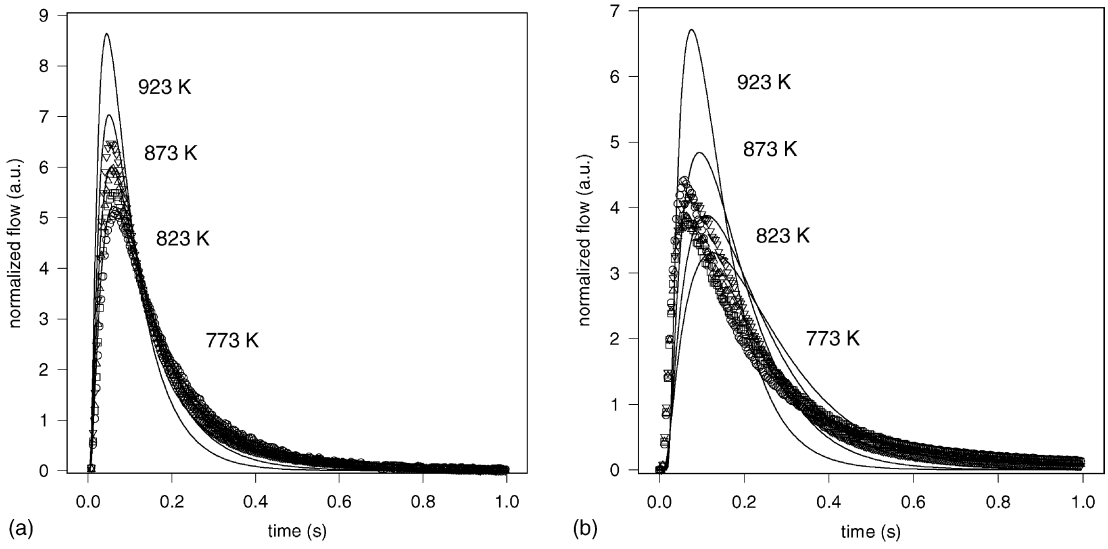

Fig. 4. Experimental and model response curves for (a) hydrogen and (b) propane produced during 2,3-methylbutane cracking from 773 to 923 K.

4. Conclusions

Although very low pressures are applied in TAP experiments, conditions far from those in a FCC unit, this transient technique offers several advantages to the study of cracking of hydrocarbons. The low pressure conditions suppress bimolecular reactions, eliminating the necessity to work at very low conversions and, thus, allowing to study the protolytic cracking in great detail. The small reactant to catalyst ratio used in the TAP reactor avoids catalyst deactivation by coke formation. Moreover, diffusion, sorption and intrinsic kinetic parameters can be readily determined from the transient response curves.

The protolytic cracking of the hexane isomers (*n*-hexane, 2-methylpentane, 3-methylpentane, 2,2-dimethylbutane and 2,3-dimethylbutane) over an industrial FCC catalyst has been analyzed in terms of product distribution and the transport, sorption and kinetic parameters have been estimated. The production of light hydrocarbons and hydrogen is a purely catalytic process as thermal reactions could be excluded under these conditions. The reactivity and product distribution of the various isomers can be explained from stability considerations of the carbenium ion formed as a result of the collapse of the carbonium ion transition state. No significant amounts of ethane and butane were observed. The protolytic attack on a C–methyl bond, producing methane, is strongly favored by the degree of substitution of the carbon atom, while the formation of hydrogen is clearly related to the possibility to form tertiary carbenium ions.

The sorption parameters have a clear relationship with molecule branching and the adsorption increases with increasing degree of branching. The micropore diffusivity is similar for all hexane isomers studied. The activation energies for the overall disappearance of the C6 paraffins vary only slightly with the degree of branching. This overall activation energy contains contributions of dehydrogenation and C–C bond cleavage. In the case of 2,2-dimethylbutane, this activation energy correspond to the cleavage of the C–C bond in the carbonium transition state leading to the formation of methane and an adsorbed carbenium ion. In the case of 2,3-dimethylbutane, a lower activation energy of $150\,kJ\,mol^{-1}$ for the formation of hydrogen was found, implying two different transition state for protolytic dehydrogenation and C–C bond breaking.

References

[1] B.S. Greensfelder, H.H. Voge, G.M. Good, Ind. Eng. Chem. 41 (1949) 2573.
[2] W.O. Haag, R.M. Dessau, in: Proceedings of the 8th International Congress on Catalysis, Vol. 2, Berlin, Verlag Chemie, Weinheim, 1984, p. 305.
[3] A. Corma, J. Planelles, J. Sanchez-Marin, F. Tomas, J. Catal. 93 (1985) 30.
[4] E.A. Lombardo, W.K. Hall, J. Catal. 112 (1988) 494.
[5] Y. Zhao, G.R. Bamwenda, B.W. Wojciechowski, J. Catal. 142 (1993) 465.
[6] D.B. Lukianov, J. Catal. 145 (1994) 54.
[7] D.B. Lukianov, J. Catal. 147 (1994) 794.
[8] G. Yaluris, J.E. Rekoske, R.J. Aparicio, R.J. Madon, J.A. Dumesic, J. Catal. 153 (1995) 54.
[9] A. Corma, P.J. Miguel, A.V. Orchilles, J. Catal. 145 (1994) 17.
[10] M. Bassir, B.W. Wojciechowski, J. Catal. 150 (1994) 1.
[11] G.R. Bamwenda, Y. Zhao, B.W. Wojciechowski, J. Catal. 148 (1994) 595.
[12] V. Fierro, J.L. Duplan, J. Verstraete, Y. Schuurman, C. Mirodatos, in: G.F. Froment, K.C. Waugh (Eds.), Reaction Kinetics and the Development and Operation of Catalytic Processes, Studies in Surface Science and Catalysis, Vol. 133, Elsevier, Amsterdam, 2001, p. 341.
[13] O.P. Keipert, M. Baerns, Chem. Eng. Sci. 53 (1998) 3623.
[14] T.A. Nijhuis, L.P.J. van den Broeke, J.M. van de Graaf, F. Kapteijn, M. Makkee, J.A. Moulijn, Chem. Eng. Sci. 54 (1999) 4423.
[15] Y. Schuurman, A. Pantazidis, C. Mirodatos, Chem. Eng. Sci. 54 (1999) 3619.
[16] J.T. Gleaves, G.S. Yablonskii, P. Phanawadee, Y. Schuurman, Appl. Catal. A: Gen. 160 (1997) 55.
[17] J.P. Huinink, J.H.B.J. Hoebink, G.B. Marin, Can. J. Chem. Eng. 74 (1996) 580.
[18] D.W. Marquardt, J. Soc. Ind. Appl. Math. 11 (1963) 431.
[19] J.A. Dumesic, D.F. Rudd, L. Aparicio, J.E. Rekoske, A.A. Teviño, The Microkinetics of Heterogeneous Catalysis. American Chemical Society, Washington, DC, 1993.
[20] B. Sowerby, S.J. Becker, L.J. Belcher, J. Catal. 161 (1996) 377.
[21] E.G. Derouane, J.B. Nagy, C. Fernandez, Z. Gabelica, E. Laurent, P. Malgean, Appl. Catal. 40 (1988) L1–L10.
[22] F. Eder, J.A. Lercher, Zeolites 18 (1997) 75.
[23] C.L. Cavalcante, D.M. Ruthven, Ind. Eng. Chem. Res. 34 (1995) 177.
[24] L. Boulicaut, S. Brandani, D.M. Ruthven, Microp. Mesop. Mater. 25 (1998) 81.
[25] R.R. Schumacher, B.G. Anderson, N.J. Noordhoek, F.J.M.M. de Gauw, A.M. de Jong, M.J.A. de Voigt, R.A. van Santen, Mesop. Microp. Mater. 35/36 (2000) 315.
[26] N. van den Beguin, L.V.C. Rees, J. Caro, M. Bülow, Zeolites 9 (1989) 287.
[27] M. Eic, D.M. Ruthven, in: P.A. Jacobs, R.A. van Santen (Eds.), Zeolites: Facts, Figures, Future, Studies in Surface Science and Catalysis, Vol. 49, Elsevier, Amsterdam, 1989, p. 897.
[28] W. Heink, J. Kärger, H. Pfeifer, K.P. Datema, A.K. Nowak, J. Chem. Soc., Faraday Trans. 88 (1992) 3505.
[29] H. Jobic, M. Bee, J. Caro, in: R. von Ballmoos (Ed.), Proceedings of 9th International Zeolite Conference, Butterworth-Heinemann, Stoneham, MA, 1993, p. 121.
[30] M. Hermann, W. Niessen, H.G. Karge, in: H.K. Beyer, H.G. Karge, I. Kiricsi, J.B. Nagy (Eds.), Catalysis by Microporous Materials, Studies in Surface Science and Catalysis, Vol. 94, Elsevier, Amsterdam, 1995, p. 131.
[31] L. Song, L.V.C. Rees, in: M.M.J. Treacy, B.K. Marcus, M.E. Bischer, J.B. Higgings (Eds.), in: Proceedings of 12th International Zeolite Conference, Materials Research Society, Warrendale, PA, 1999, p. 67.
[32] M.A. Jama, M.P.F. Delmas, D.M. Ruthven, Zeolites 18 (1997) 200.
[33] J. Xiao, J. Wei, Chem. Eng. Sci. 47 (1992) 1143.
[34] J.A. Lercher, R.A. van Santen, H. Vinek, Catal. Lett. 27 (1994) 91.
[35] T.F. Narbeshuber, H. Vinek, J.A. Lercher, J. Catal. 157 (1995) 388.
[36] W.O. Haag, Stud. Surf. Sci. Catal. (1994) 1375.
[37] S.M. Babitz, B.A. Williams, J.T. Miller, R.Q. Snurr, W.O. Haag, H.H. Kung, Appl. Catal. A: Gen. 179 (1999) 71.
[38] A.F.H. Wielers, M. Vaarkamp, M.F.M. Post, J. Catal. 127 (1991) 51.
[39] A.I. Biaglow, D.J. Parillo, G.T. Kokotailo, R.J. Gorte, J. Catal. 148 (1994) 213.
[40] A. Brait, K. Seshnan, H. Weinstabl, A. Ecker, J.A. Lercher, Appl. Catal. A: Gen. 169 (1998) 313.
[41] Y.X. Zhao, B.W. Wojciechowski, J. Catal. 163 (1996) 365.
[42] NIST Chemistry Webbook, http://webbook.nist.gov/chemistry/.